PROCEEDINGS OF SCIENCE

Review of ATLAS Heavy Quark and Quarkonium results

Miriam WATSON*
University of Birmingham
E-mail: Miriam.Watson@cern.ch
on behalf of the ATLAS Collaboration

Several recent results from the ATLAS experiment at the Large Hadron Collider are presented, using proton-proton collisions at $\sqrt{s} = 7$ TeV. A new measurement of the differential production cross-section of B^+ mesons in the region $|\eta| < 2.25$ and $9 < p_T < 120$ GeV is described, together with the differential cross-sections of b-hadrons via the decay mode $D^{*+}\mu^- X$. Comparisons with next-to-leading-order and fixed-order-next-to-leading-logarithm predictions are made. Recent studies performed by ATLAS on the production of Υ(nS), n=1, 2, 3, in the region $|y| < 2.3$ and $p_T < 70$ GeV are shown. Theoretical production models are compared to differential cross-sections and cross-section ratios for Υ(nS). Finally, the associated production of quarkonia and vector bosons is discussed as a novel method for comparing colour singlet and colour octet production models. Results on $J/\psi + W$ production are presented.

The European Physical Society Conference on High Energy Physics -EPS-HEP2013
18-24 July 2013
Stockholm, Sweden

*Speaker.

PoS(EPS-HEP 2013)468

1. Introduction

The production of heavy quarks at hadron colliders allows the validity of quantum chromodynamics (QCD) predictions and calculations to be tested. Measurements of the b-hadron production cross-sections in proton-proton collisions at the Large Hadron Collider provide tests of QCD calculations at higher centre-of-mass energies and in wider transverse momentum (p_T) and rapidity (y) ranges than before. In addition, measurements of the properties of heavy quark-antiquark bound states, or quarkonia, provide a unique insight into the nature of QCD close to the strong decay threshold and should allow discrimination between different theoretical approaches.

In this report, recent results from the ATLAS experiment on heavy flavour production cross-sections and quarkonium physics are presented and compared with theoretical predictions.

2. The ATLAS detector and performance

A detailed description of the ATLAS detector can be found in Ref.[1]. The components of the detector that are critical for heavy flavour measurements are the inner tracking detector, for precise position information, and the muon chambers, which comprise both tracking and triggering detectors. The inner and muon detectors have solenoidal and toroidal magnetic fields, respectively, to provide momentum information. Some analyses use the ATLAS calorimetry in addition, for identification of photons or the calculation of missing transverse energy. The period of data-taking between 2010 and 2012 was very successful, with a total of over 25 fb^{-1} recorded for physics analyses. The results presented here use the 2010–2011 data samples at a centre-of-mass energy of 7 TeV. Heavy flavour decays are selected using muon signatures, often involving J/ψ or Υ decays. These events are preselected using single- or di-lepton triggers, including dedicated di-muon triggers with high efficiency for J/ψ, Υ or B meson decays.

3. Cross-sections for b-hadron and B^+ meson production

The b-hadron (H_b) cross-section is measured in the 2010 dataset using the partially reconstructed decay mode $D^{*+}\mu^- X$, where D^{*+} decays via $D^{*+} \to \pi D^0 (\to K^-\pi^+)$ (and charge conjugate) [2]. The invariant mass difference between the D^{*+} and D^0 decay products is fitted as a function of the $D^{*+}\mu$ transverse momentum, p_T, and pseudorapidity, η, then the measured yield is corrected for fiducial acceptance and unfolded for unobserved b-hadron decay products. The differential H_b cross-sections for $p_T(\mathrm{H_b}) > 9$ GeV and $|\eta(\mathrm{H_b})| < 2.5$ are compared with next-to-leading order (NLO) predictions in Fig. 1. The data are seen to lie slightly above POWHEG [3] and MC@NLO [4], although the difference is within the combined experimental and theoretical uncertainties, where the latter are dominated by the scale uncertainty.

The B^+ meson cross-section has been evaluated in the $J/\psi K^+$ decay channel (and charge conjugate), using 2.4 fb^{-1} of data from the 2011 run [5]. Reconstructed $J/\psi \to \mu^+\mu^-$ candidates in the mass window [2.7, 3.5] GeV are combined with an additional inner detector track (the kaon candidate) and fitted to a common vertex. Kinematic cuts are applied and $B^\pm$ candidates with $p_T > 9$ GeV and $|y| < 2.25$ are retained.

The differential cross-sections for B^+ are extracted from fits to the $J/\psi K^\pm$ mass distribution, taking into account the resonant backgrounds from $J/\psi\pi$ and $J/\psi K\pi$, as well as combinatorial

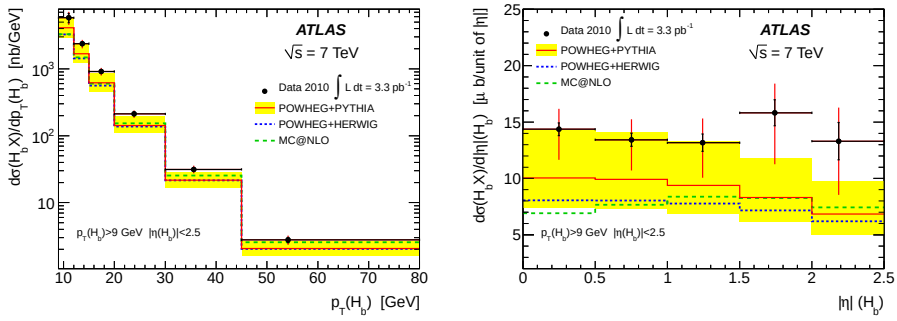

Figure 1: Differential b-hadron (H_b) cross-section as a function of p_T (left) and $|\eta|$ (right) [2].

background from J/ψ+X. An example is shown in Fig. 2 (left). Corrections are applied for detector acceptance, trigger efficiency and $B^{\pm}$ reconstruction efficiencies.

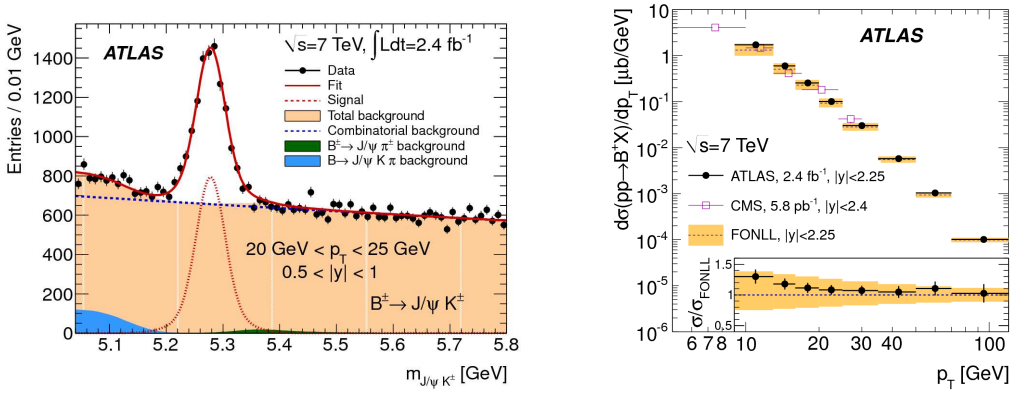

Figure 2: Invariant mass of $B^+ \to J/\psi K^+$ candidates (left) and differential B^+ cross-section (right) [5].

The differential B^+ cross-section is shown in Fig. 2 (right) as a function of p_T, integrated over the full rapidity range. There is good agreement between the ATLAS and CMS measurements [6] where they overlap, at lower p_T. The plot also shows the prediction of the fixed-order-next-to-leading-logarithm calculation, FONLL [7], assuming the world average hadronisation fraction to B^+ [8]. The prediction is in good agreement with the data, within the theoretical uncertainties.

The double-differential B^+ meson cross-section is displayed in Fig. 3 (left) for a range of rapidities and for transverse momenta up to 120 GeV. The same information is displayed in Fig. 3 (right) for each rapidity bin as a function of p_T, for the ratio of data divided by the NLO predictions of POWHEG [3] and MC@NLO [4]. The measurement uncertainties are shown on the data points, and the theoretical uncertainties as shaded bands. POWHEG describes the data well throughout the distributions, but MC@NLO underestimates the cross-section at low p_T. It predicts a p_T spectrum that is slightly softer than the data for low rapidities, and slightly harder at higher rapidities.

The integrated B^+ production cross-section in the kinematic range 9 GeV $< p_T <$ 120 GeV and $|y| < 2.25$ is measured to be $\sigma(pp \to B^+X) = 10.6 \pm 0.3(\text{stat.}) \pm 0.7(\text{syst.}) \pm 0.2(\text{lumi.}) \pm 0.4(\mathscr{B})$ μb, in agreement with theoretical predictions.

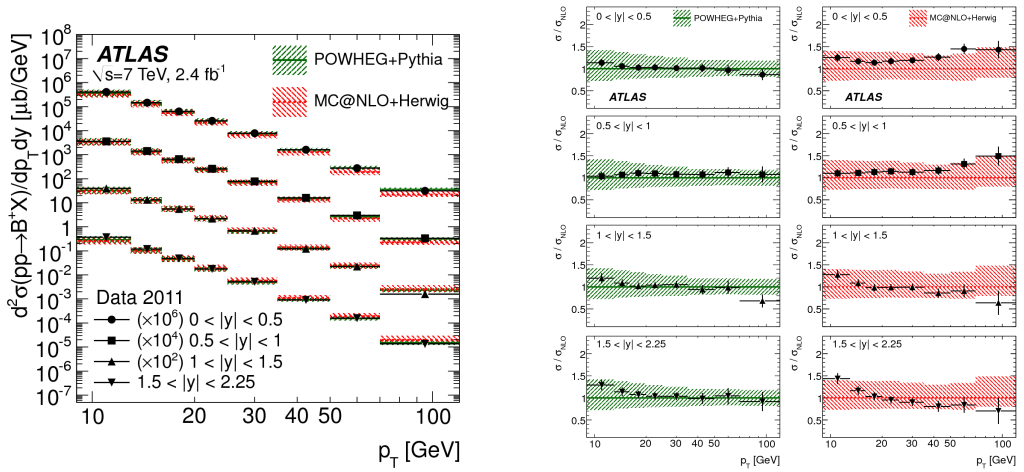

Figure 3: Double-diffential cross-section of B^+ production as a function of p_T and y (left), and ratio of data to the NLO predictions of POWHEG and PYTHIA (right) [5].

4. Bottomonium production: Υ and χ_b

The remainder of this report will cover recent measurements of the quarkonium sector at ATLAS. Various QCD mechanisms can contribute to quarkonium production, such as colour singlet and colour octet processes, and improved experimental measurements will help to provide new insight into the production mechanism.

Production cross-sections and relative ratios of $\Upsilon(1S,2S,3S)$ have been measured in 1.8 fb^{-1} of data recorded in 2011, via the decay channel $\Upsilon \to \mu^+\mu^-$ [9]. The measurement of Υ production follows a similar procedure to the B^+ cross-section: the dimuon invariant mass distribution is fitted in fine bins of transverse momentum and rapidity, with corrections for trigger and reconstruction efficiencies and detector acceptance, to extract differential cross-sections. The fiducial acceptance correction has a dependence on the spin alignment of the Υ; the central value of the measurements assumes an isotropic angular distribution for the muons, but other spin alignment scenarios have been considered.

The corrected differential distribution for $\Upsilon(1S)$ is shown in Fig. 4 (left) for the central rapidity region, $|y| < 1.2$, in comparison with the predictions of two QCD models (see Ref. [9] for details). The first is a next-to-next-to-leading-order colour singlet prediction (CSM), which contains only direct Υ production, with no feed-down from other states. The second prediction is a more phenomenological model known as colour evaporation (CEM), which includes all Υ production. Both models agree reasonably well with the measured distribution at low p_T, where data from the Tevatron were already available, but fail to describe the shape or normalisation overall. Similar behaviour is found at larger rapidities and for $\Upsilon(2S,3S)$. The spin alignment uncertainty, shown as a blue band, becomes negligible at high p_T.

Another interesting measurement is to compare the cross-section ratios of $\Upsilon(2S)$ or $\Upsilon(3S)$ to $\Upsilon(1S)$. Figure 4 (right) shows the ratios as a function of $p_T(\Upsilon)$ for the central rapidity region, where the hashed bands give the total uncertainty, excluding spin alignment effects. The initial rise with p_T indicates that the production rates of the 2S and 3S states are increasing with p_T, but then

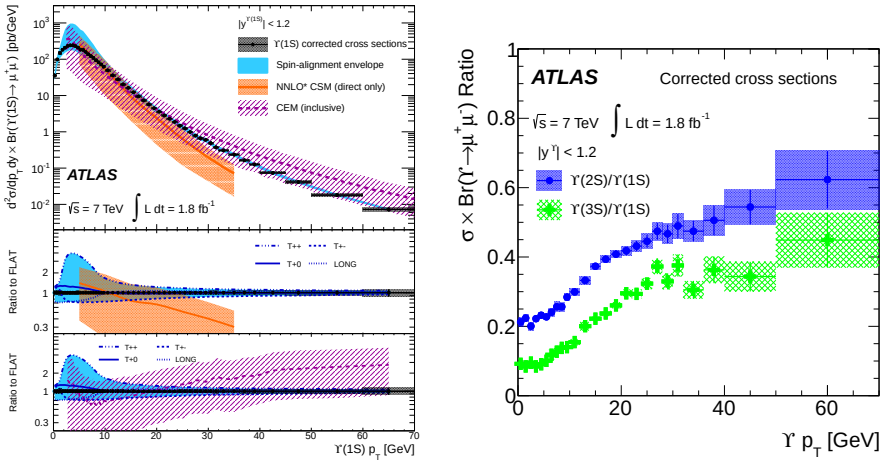

Figure 4: Differential cross-section for $\Upsilon(1S)$ production (left) and ratios of differential cross-sections $\Upsilon(2S)/\Upsilon(1S)$, $\Upsilon(3S)/\Upsilon(1S)$ (right), each multiplied by the di-muon branching fractions [9].

there is a hint of saturation at higher p_T, where perhaps direct production dominates over decays of excited states. In contrast, there is little dependence on rapidity for the production ratios.

The relative production rates for $\Upsilon(nS)$ will depend on feed-down contributions from the P-wave χ_b states. The $\chi_b(3P)$ state was observed for the first time in ATLAS through its radiative decays to $\Upsilon(1S)$ and $\Upsilon(2S)$ [10]. Recent measurements of the $\chi_b(3P)$ and theoretical predictions are summarised in Fig. 5 (left) [11]. The new state lies just below the $B\bar{B}$ threshold and must be taken into account in theoretical predictions of Υ properties.

5. Associated production of W bosons and prompt J/ψ

The associated production of a W boson and a prompt J/ψ meson provides a powerful probe of charmonium production and may be able to distinguish between colour-singlet and colour-octet contributions. This signature will also be sensitive to multiple parton interactions, and the current measurement includes an estimate of the double parton scattering (DPS) contribution [12].

Using 4.6 fb^{-1} of data, the J/ψ and $W^{\pm}$ are both identified in their muon decay modes: $J/\psi \to \mu^+\mu^-$ and $W \to \ell\nu$, using a high-p_T single muon trigger. The J/ψ invariant mass and pseudo-proper time, shown in Fig. 5 (centre, right) are fitted simultaneously to extract the prompt J/ψ component. Each prompt candidate then receives a weight in the W transverse mass distribution. The transverse mass is fitted with W and multi-jet templates, and the jet contamination is estimated to be 0.1 ± 4.6 events. In total, $29.2^{+7.5}_{-6.5}$ associated W boson and prompt J/ψ candidates are found in the data, allowing the background-only hypothesis to be rejected at 5.3σ.

The DPS contribution is estimated under the assumption that the $W^{\pm}$ and J/ψ processes are independent and uncorrelated, using both the ATLAS prompt J/ψ cross-section [13] and an effective cross-section obtained from $W(\to \ell\nu) + 2$ jet events [14]. These assumptions give an estimated DPS contribution of around 40%. The azimuthal angle between the W and the J/ψ is expected to be uniform for DPS, but should peak around π for single scattering events (SPS). This quantity is shown in Fig. 6 (left) and supports the presence of both components in the data.

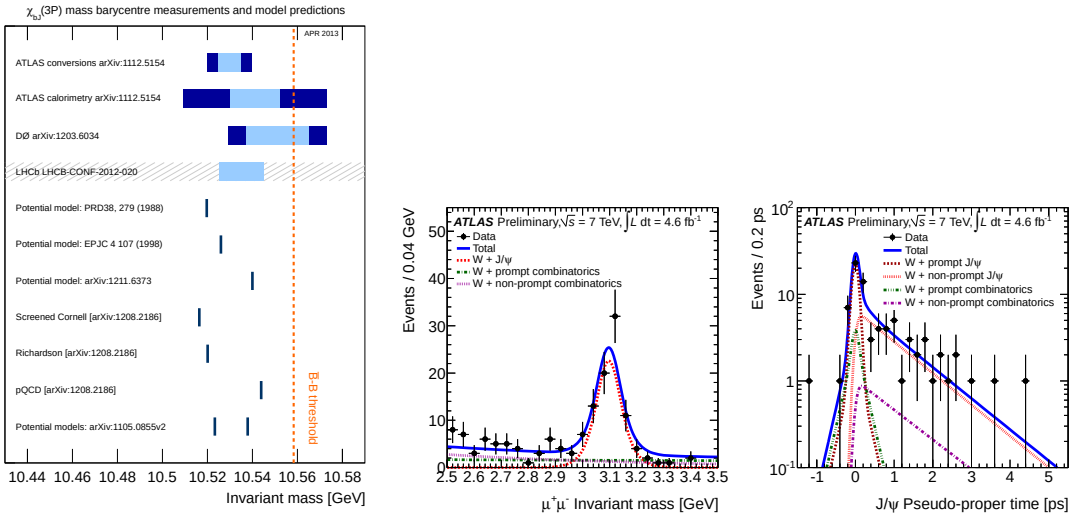

Figure 5: Summary of $\chi_b(3P)$ measurements and predictions (left), where the light and dark bands show statistical and total uncertainties [10, 11]; J/ψ invariant mass (centre) and pseudo-proper time (right) in the $W + J/\psi$ analysis [12].

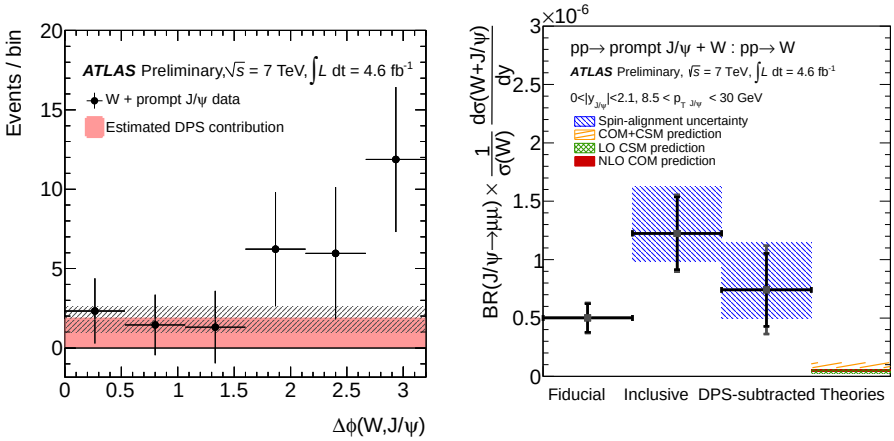

Figure 6: Azimuthal angle between the J/ψ and W (left), where the hashed region shows the uncertainty on the DPS estimate; cross-section ratio of $W + J/\psi$ to inclusive W production (right) [12].

The $W + J/\psi$ cross-section is measured relative to the inclusive W cross-section in the same dataset. Fig. 6 (right) shows the cross-section ratio under various assumptions: firstly, a fiducial measurement, then corrected for J/ψ acceptance, and then with the estimated DPS contribution subtracted. This third bin gives an estimate of the cross-section ratio for SPS. The SPS predictions of two models are also shown: a leading-order colour singlet model [15] and next-to-leading order colour octet model [16], and their sum. These predictions currently lie much lower than the data, but within 2σ of the large measurement uncertainties. Updated calculations and comparisons with the data are expected to be available soon.

6. Summary

Recent ATLAS measurements of heavy flavour production cross-sections and quarkonium

properties in both the charm and bottom sector are presented. The discovery of the $\chi_b(3P)$ has an important interplay with measurements and predictions of Υ production, and the first observation of associated vector boson and prompt J/ψ production opens a new field in understanding both quarkonium production and multiple parton interactions.

Acknowledgments

The author is supported by a Royal Society Research Fellowship.

References

[1] ATLAS Collaboration, *The ATLAS Experiment at the CERN Large Hadron Collider*, JINST **3** (2008) S08003.

[2] ATLAS Collaboration, *Measurement of the b-hadron production cross section using decays to $D^*\mu X$ final states in pp collisions at $\sqrt{s} = 7$ TeV with the ATLAS detector*, Nucl. Phys. **B864** (2012) 341, [arXiv:1206.3122].

[3] P. Nason, *A new method for combining NLO QCD with shower Monte Carlo algorithms*, JHEP **11** (2004) 040, [hep-ph/0409146].

[4] S. Frixione and B. R. Webber, *Matching NLO QCD computations and parton shower simulations*, JHEP **06** (2002) 029, [hep-ph/0204244].

[5] ATLAS Collaboration, *Measurement of the differential cross-section of B^+ meson production in pp collisions at $\sqrt{s} = 7$ TeV at ATLAS*, Submitted to JHEP, [arXiv:1307.0126].

[6] CMS Collaboration, *Measurement of the B^+ production cross section in pp collisions at $\sqrt{s} = 7$ TeV*, Phys. Rev. Lett. **106** (2011) 112001, [arXiv:1101.0131].

[7] M. Cacciari et al., *Theoretical predictions for charm and bottom production at the LHC*, JHEP **10** (2012) 137, [arXiv:1205.6344].

[8] Particle Data Group, J. Beringer et al., *Review of Particle Physics*, Phys. Rev. **D86** (2012) 010001.

[9] ATLAS Collaboration, *Measurement of Upsilon production in 7 TeV pp collisions at ATLAS*, Phys. Rev. **D87** (2013) 052004, [arXiv:1211.7255].

[10] ATLAS Collaboration, *Observation of a New χ_b State in Radiative Transitions to $\Upsilon(1S)$ and $\Upsilon(2S)$ at ATLAS*, Phys. Rev. Lett. **108** (2012) 152001, [arXiv:1112.5154].

[11] D. Price for the ATLAS Collaboration, compilation for DIS2013, [ATL-PHYS-SLIDE-2013-221].

[12] ATLAS Collaboration, *Measurement of the production cross section of prompt J/ψ mesons in association with a $W^{\pm}$ boson in pp collisions at $\sqrt{s} = 7$ TeV*, [ATLAS-CONF-2013-042].

[13] ATLAS Collaboration, *Measurement of the differential cross-sections of inclusive, prompt and non-prompt J/ψ production in proton-proton collisions at $\sqrt{s} = 7$ TeV*, Nucl. Phys. **B850** (2011) 387, [arXiv:1104.3038].

[14] ATLAS Collaboration, *Measurement of hard double-parton interactions in $W(\rightarrow \ell\nu) + 2$ jet events at $\sqrt{s} = 7$ TeV with the ATLAS detector*, New J. Phys. **15** (2013) 033038, [arXiv:1301.6872].

[15] J. P. Lansberg and C. Lorce, *Reassessing the importance of the colour-singlet contributions to direct $J/\psi + W$ production at the LHC and the Tevatron*, [arXiv:1303.5327].

[16] G. Li et al., *QCD corrections to J/ψ production in association with a W-boson at the LHC*, Phys. Rev. **D83** (2011) 014001, [arXiv:1012.3798].